Experimental and numerical study of globe valve housing

Nenad R. Mitrovic[1], Aleksandar Lj. Petrovic[1], Milos S. Milosevic[2], Nikola V. Momcilovic[1], Zarko Z. Miskovic[1], Tasko Dj. Maneski[1], Predrag S. Popovic[3]

[1]University of Belgrade, Faculty of Mechanical Engineering, Belgrade, Serbia
[2]University of Belgrade, Innovation Center of Faculty of Mechanical Engineering, Belgrade, Serbia
[3]University of Belgrade, Vinča Institute of Nuclear Sciences, Belgrade, Serbia

Abstract

Complex structure experimental analysis has always been a huge challenge for researchers. Conventional experimental methods (*e.g.*, strain gauges) give only limited data sets regarding measurement on critical areas with high geometrical discontinuities. A 3D Digital Image Correlation method is an optical method that overcomes the limitations of conventional methods and enables full-field displacement and strain measurement of geometrically complex structures. System Aramis, based on Digital Image Correlation method, is used for experimental analysis and numerical model verification in this paper. Investigated complex structure is sphere/cylinder junction on globe valve housing subjected to axial loading. The highest experimentally measured von Mises strain values around 0.15% are recorded on cylinder/sphere intersection. Von Mises strain values on cylindrical and spherical part are several times smaller than on intersection itself. It is important to emphasize that, to the authors' best knowledge, this is the first paper showing experimental results of 3D full and strain field of geometrically complex structure (sphere/cylinder intersection) on the intersection itself on pressure equipment. It is proven that 3D Digital Image Correlation method is fast and versatile method for recording strain during loading of complex structures.

Keywords: geometrical discontinuity, globe valve housing, 3D digital image correlation method, finite element analysis, sphere/cylinder junction, axial loading.

A valve, as a device for regulating the flow of a fluid, comes in various designs for the use in chemical industry. The valve designs depend on the fluid being handled, the nature of control or the application desired as well as temperature and pressure [1]. In the chemical industry, valves are confronted with high requirements towards safety and reliability, so the strength of the valve housing is of great importance. One of the most commonly used valves in chemical industry is globe valve. Typical globe valve housing has complex structure, a geometrical discontinuity that consists of sphere/cylinder intersection.

Previous studies in the field of pressure equipment [28], *i.e.*, measuring and determining stress and strain of geometrically complex structures (sphere/cylinder intersection), have relied on analytical calculations based on shell theory, numerical calculations using computer software and conventional experimental methods. As one of the most often conclusions in their work, the researchers indicated the lack of adequate experimental data in the available literature, *i.e.*,

expressed the need for detailed experimental analysis of critical areas where is not possible to precisely determine displacement, strain and stress values using analytical or numerical models.

Limitations of conventional experimental methods were recognized in several aspects. First, standardized specimens with discontinuities were used to analyze geometrical discontinuities through tensile testing. Based on the results of tensile testing, stress concentration factors (*SCF*) were plotted on diagrams and later used to solve problems on geometrically complex structures. This approach gave only approximate solutions that are not sufficiently precise and accurate. Second, experiments were conducted using conventional methods. Limitation of conventional methods is local measurement, *i.e.*, experimental values are measured only in a single point. Third, measurements were carried out close to the geometrical discontinuity, rather than on the actual intersection of geometrical shapes, so it was not possible to measure the highest strain values.

The 3D Digital Image Correlation (DIC) [9–11] method overcomes limitations of conventional experimental methods (*e.g.*, strain gauge) and enables full-field displacement and strain measurement. One experimental measurement enables acquisition of large datasets that replaces large number of strain gauges

and significantly reduces experiment preparation time and therefore the costs. On the other hand, as finite element method calculates full displacement and strain fields, numerical model verification is easily carried out by comparing to experimental results presented in the same manner. Full strain field experimental measurement allows accurate determination of critical areas, i.e. areas with highest strain values, as well as principle stress directions that enables better theoretical analysis of complex structures. The 3D DIC method has high accuracy (up to 1 μm) and can be used in a variety of ways: testing of different materials [12–17], structure testing [18–21], model verification [21–25], fracture mechanics [26,27], etc. However, to the authors' best knowledge very few publications are available in the literature that addresses the issue of full-field experimental analysis of complex structure, *i.e.*, sphere cylinder junction on pressure equipment. Generally, full-field measurements constitute an opportunity to bridge the gap between experiments and simulations allowing for direct displacement and strain comparisons [28].

The aim of this paper is to analyze complex structure, *i.e.*, sphere/cylinder intersection subjected to axial loading using full-field experimental 3D DIC method and numerical strain and stress data.

MATERIALS AND METHODS

Geometrically complex structure tested in this paper is globe valve housing. Experimental analysis was performed on globe valve housing DN32, PN6 for axial force of 30 kN acting in the direction of valve symmetry axis (compression). Maximal axial force is force acting as pipeline dilatation influence for temperature difference of 90 °C. Area of interest, sphere/cylinder intersection, is shown in Figure 1b. Globe valve housing material is GG25 (EN GJL-250).

Valve housing was tested in tensile testing machine Zwick HB250 (Zwick, Germany) for maximal test loads up to 250 kN. Globe valve housing was placed on the T-slot table and compressed using integrated travel measurement system (Figure 1a). Axial loading was applied directly to the valve flange (Figure 1b).

Strain fields were measured using 3D system Aramis 2M (GOM, Germany) based on DIC method. System consists of two cameras (50 mm camera lenses), camera stand and computer. Aramis setup parameters were as follows: measuring volume was 105 x 80 x 55 mm, measuring distance 800 mm, calibration panel CP 20/90/D07210 and calibration deviation was 0,038. Custom made LED lamp was used as lighting. Experimental setup – valve, cameras and testing machine are shown in Figure 1c.
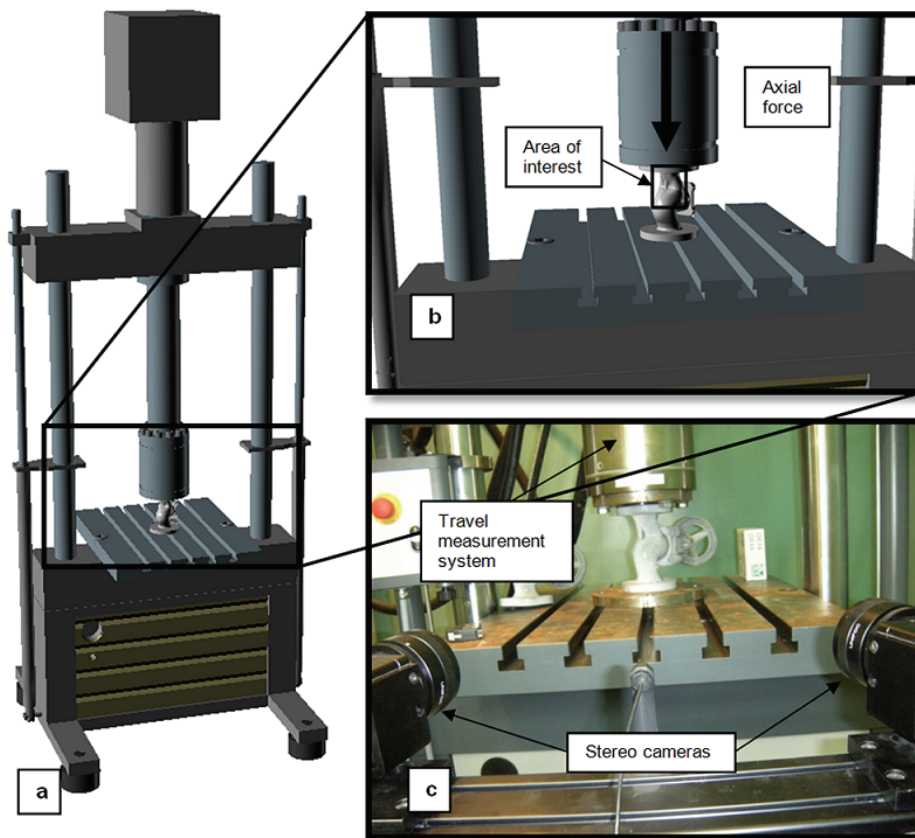

Figure 1. Experiment. a) Valve position on tensile testing machine. b) Area of interest on valve housing. c) Experimental setup.

Experimental procedure

For system for 3D optical strain measurement application on complex structure problems, appropriate procedures are defined and developed (operations before testing, during testing and after testing and result processing).

Experiment was conducted according to following procedure.

Sample preparation. The surface of the measuring object must have a pattern with good contrast in order to clearly allocate the pixels in camera images. Valve housing surface was cleaned and sprayed for the experiment. White paint was sprayed as base color for black dots stochastic pattern used as reference points for Aramis system analysis.

Selection of measuring volume. Selection of measuring volume was based on the size of the sample and the area of interest on the sample.

System calibration. Prior to experiment, Aramis calibration was performed for chosen measuring volume using calibration panel CP 20/90/D07210. Calibration panel corresponds to chosen measuring volume. During calibration, sensor configuration is determined. This means that distance and orientation of the cameras to each other are determined.

Sample positioning. Valve housing was positioned vertically and coaxially to integrated travel measurement system movement. Integrated travel measurement system positioning was done automatically, limiting the contact force with valve flange below 0.05 kN.

Measurement. After successful calibration, measurement was performed. Housing was gradually loaded, with force increasing 0.2 kN/s. Maximal experimental loading was 30.1 kN. Digital images were automatically recorded immediately before, every 5 s during the loading and immediately after unloading. First recorded image pair (before the loading) are reference images for data processing. Number of recorded image pairs is 32.

Data processing. Afterwards, computation was performed by Aramis. After computation, additional data processing was also done in softwares Origin and Statistica.

During the experiment, system automatically defined global coordinate system. The position of the coordinate system depends on the calibration of the cameras and usually has no logical relation to the specimen. The coordinate system allows for unambiguously describing the position of points in the 3D space by stating three numerical values (*X*,*Y*,*Z* coordinates). Depending on the measurement task, the strain and displacement data of a measuring project should be transformed into a defined coordinate system in order to be interpreted correctly. One of the mostly used methods for coordinate system transformation that has been used in this paper is 3-2-1 Transformation. 3-2-1 means that three 3D points (*Z*1, *Z*2, *Z*3, located as far as possible from each other and not in a line) describe a plane, two additional 3D points describe a line (*Y*1, *Y*2, located as far as possible from each other in the *X*-axis) and one 3D point describes a point (*X*). For the transformation method *ZZZ-YY-X* means the following: three *Z* points (*Z*1, *Z*2, *Z*3) define the *Z*-plane, the additional two *Y* points (*Y*1, *Y*2) define the *Y*-plane and the *X* point defines the *X*-plane. At the intersection of the planes is the zero point of the coordinate system. For easier result analysis, new global coordinate system is defined with origin positioned on the sphere/cylinder intersection and *Y*-axis in axial force direction. 3D strain field was measured on the sphere/cylinder intersection.

Numerical model

Finite element method (FEM) is used as a tool for numerical analysis of the globe valve behavior under axial load. FEM software package used in this paper is Abaqus. FEM model consists of 40001 solid tetrahedral elements and 62584 nodes. Mesh density is increased in areas where geometric discontinuities occur and where stress concentration is expected in order to obtain the most accurate results from the model. The direction of the force representing axial dilatations and the analyzed area of interest corresponds to experimental analysis (Figure 2c). Applied load and model geometry are symmetrical, so only one half of the model is analyzed and presented. The numerical model represented actual experimental conditions: axial load
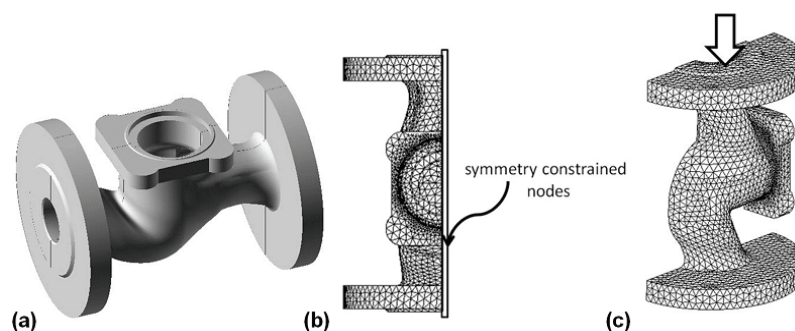

Figure 2. Numerical model. a) Valve numerical model. b) Model symmetry plane. c) Model loading.

up to 30 kN, supported flange and symmetry constraints of nodes in the symmetry plane (Figure 2b). All the nodes located on the symmetry plane have displacement constrained in transverse direction [13] and rotation constrained in other two directions. Mechanical properties of material GG25 (EN GJL-250) are: 0.1% proof stress is 165 MPa, tensile strength is 250 MPa and modulus of elasticity is 110 kN/mm^2.

RESULTS AND DISCUSSION

Von Mises strain results are presented in this paper. Strain field was analyzed using four sections (sections 1–4), as shown in Figure 3. Sections 1–3 are positioned vertically at distance of 8 mm from each other. Section length is around 80 mm and every section consists of around 65 points. Section 4 is positioned horizontally on sphere cylinder intersection. Section 4 length is around 26 mm. Experimental data is also presented graphically as function of section length.

Von Mises strain results for maximum axial force of 30 kN are shown in Figure 3. Scale in % is given on ordinate of Figure 3. The 3D Von Mises strain field across the sample surface (Figure 3c and d) is showing the highest measured strains (yellow color), around 0.15%, in the area of highest geometrical discontinuity, *i.e.*, on sphere/cylinder intersection. Von Mises strain values are also given as section length function (Figure 3a and b). Sharp peaks on Sections 1–3 correspond to the position of sphere/cylinder intersection (Figure 3d). Sections 1–3 have the same trend, but strain values are

decreasing respectively as the geometrical discontinuity is decreasing by moving away from Section 1 towards Section 3. This trend is more obvious on Section 4 (Figure 3b), where constant strain reduction can be observed.

Von Mises strain values on the housing spherical and cylindrical part are below 0.05%. Von Mises strain values on housing spherical and cylindrical part are several times smaller than on the sphere/cylinder intersection. Von Mises strain values have a slight increase in the initial part of Section 1 length, as influence of discontinuity due to flange connection.

The 3D DIC method has some limitations. As the 3D computation of the measuring points is based on pixels that need to be seen from the right and left camera with the individual facet pattern, a correct 3D computation and strain computation is not possible for sample edges. So high strain values (red color) that can be seen on strain field edges represent system errors and are not taken into consideration. Results shown on diagram for Section 4 (Figure 3b), for section length after 21 mm, are also not taken into consideration as that area cannot be correctly seen by both cameras.

Experimental Von Mises strain values for Section 4 were also plotted as a function of section length and strain stage (Figure 4). Strain stages (0–30) represent force increase, where stage 0 represents beginning of the experiment prior to loading and stage 30 maximum loading force for the experiment. The 3D surface visually shows Von Mises strain increase during the loading. Sharp peaks on section length 0 for several stages rep-
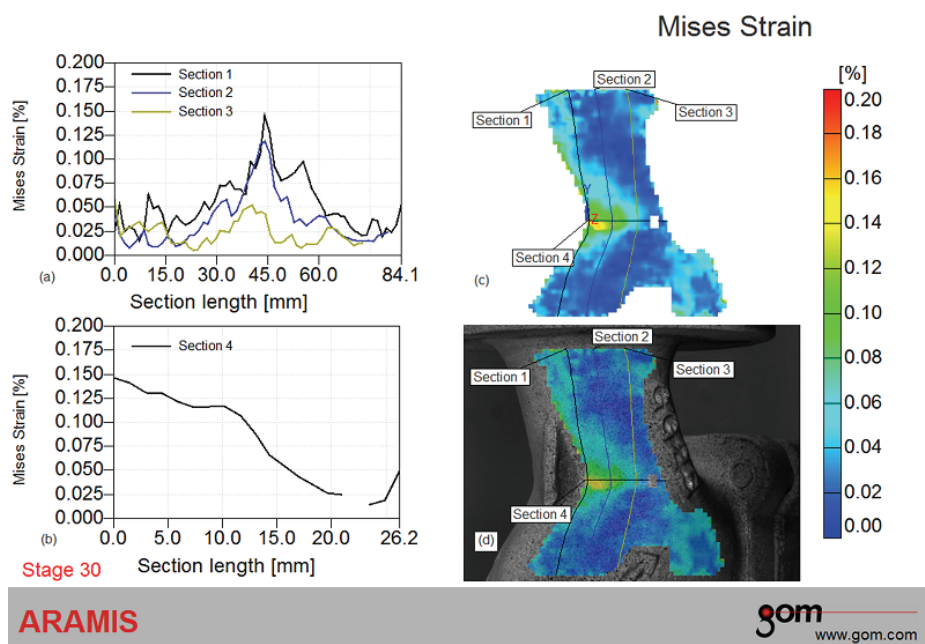

Figure 3. Experimental Von Mises strain for maximum force of 30 kN. a) Von Mises strain as a function of distance for Sections 1–3. b) Von Mises strain as a function of distance for Section 4. c) Von Mises strain field. d) Sample photograph with overlaying Von Mises strain field.
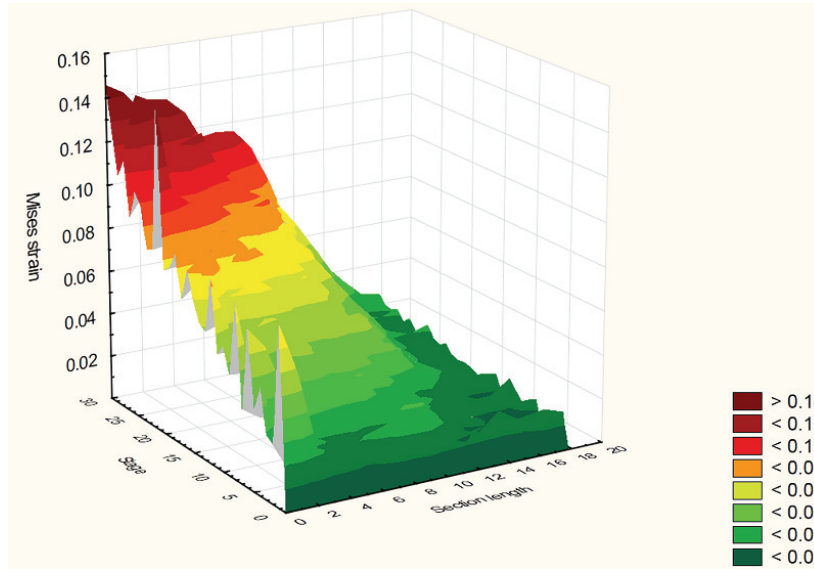
Figure 4. Experimental Von Mises strain for Section 4.

resent system errors and shouldn't be taken into consideration.

Figure 5 shows numerical results in the area of interest for maximum force of 30 kN. Von Mises strain field is shown in Figure 5a where scale on the ordinate, multiplied by 100, is showing percentage values. Highest Von Mises strain values in the area of sphere/cylinder intersection are around 0.13%. Von Mises stress field is shown in Figure 5b and scale in MPa is given on ordinate. Highest Von Mises stress values in the area of sphere/cylinder intersection are around 164 MPa.

Maximal Von Mises strain numerical (0.13%) and experimental results (0.15%) at sphere/cylinder junction for the same maximum force of 30 kN differ around 15%. Measured experimental Von Mises strain values at spherical and cylindrical part are in range of 0.02 to 0.05%. In the same region, numerical Von Mises strain results are in range of 0.00324 to 0.0410%. Maximal numerical Von Mises stress values of around 164 MPa are close to the material's proof stress (165 MPa) from the material standard. Although the proof stress in the standard represents the minimal stress value, it can be concluded that plastic deformation occurred on the valve housing under loading presented in this paper.

Experimental and numerical Von Mises strain values for Sections 1 and 2 for maximum axial force of 30 kN are shown in Figure 6. Experimental Sections 1 and 2 in Figure 6 present maximal strain values shown in Figure 3a, *i.e*., Sections 1 and 2 are connecting highest peak values. Numerical results for Section 2 (green line) are
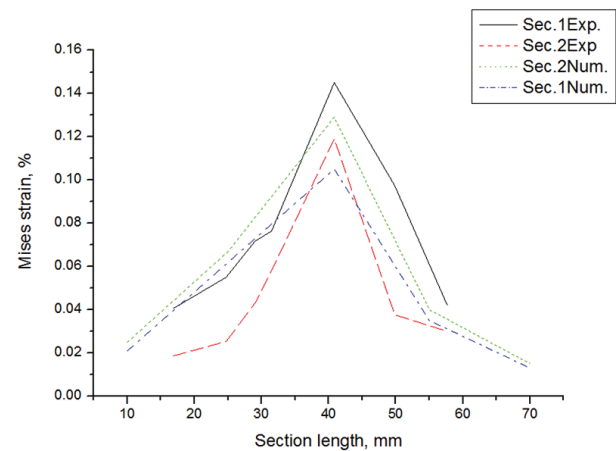

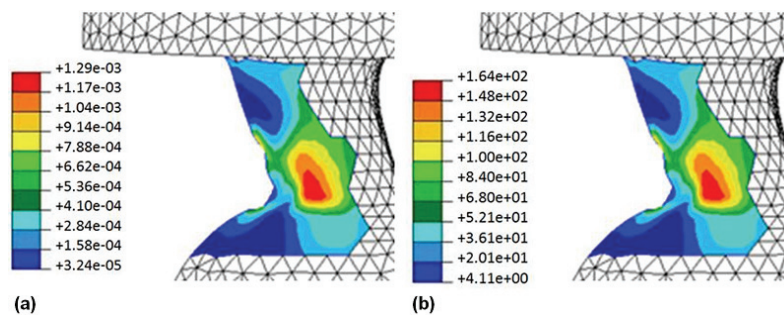*Figure 6. Experimental and numerical Von Mises strain for Sections 1 and 2.*

Figure 5. Numerical results for maximum force of 30 kN. a) Von Mises strain field. b) Von Mises stress field.

showing higher maximal strains than for Section 1 (blue line). Area of highest strain values in numerical analysis is few millimeters moved away from the reinforcement comparing to experimental results (Figures 3 and 5). Both experimental and numerical sections have the same trend, with a slightly higher strains recorded on cylindrical side of the housing.

CONCLUSIONS

In this paper, sphere/cylinder intersection subjected to axial loading was analyzed using full-field experimental DIC method and numerical data. It is important to emphasize that strain field was experimentally measured not only on spherical and cylindrical part of valve housing, but also on sphere/cylinder intersection. To the authors' best knowledge, full-field experimental results for sphere/cylinder intersection on pressure equipment are not available in the literature.

Qualitative comparison of experimental and numerical results shows that the strain distribution patterns and strain values differences in junction area are satisfactory. Maximal Von Mises strain numerical (0.13%) and experimental results (0.15%) at sphere/cylinder junction for the same maximum force of 30 kN differ around 15%. This way, satisfactory results for 3D DIC and FEM proves that methods were mutually verified.

Maximal numerical Von Mises stress values of around 164 MPa are close to the material's proof stress and plastic deformation occurred on the valve housing under axial loading of 30 kN, so elasto-plastic analysis of the valve housing should be included in the further studies.

Acknowledgments

REFERENCES

[1] S. Maidragi, Chemical process equipment: design and drawing. Volume I, PHI Learning Private Limited, Delhi, 2016.

[2] S. Schindler, J. Zeman, Stress concentration factors of nozzle–sphere connections, Int. J. Press. Vessel. Pip. **80** (2003) 87–95.

[3] V. Skopinsky, A. Smetankin, Parametric study of reinforcement of pressure vessel head with offset nozzle, Int. J. Press. Vessel. Pip. **80** (2003) 333–343.

[4] I. Galić, Z. Tonković, K. Vučković, Experimental and Numerical Investigation of Collapse and Burst Pressures for a Valve Housing, Strain **47** (2011) 519–524.

[5] H. Al-Gahtani, A. Khathlan, M. Sunar, M. Naffa'a, Local pressure testing of spherical vessels, Int. J. Press. Vessel. Pip. **114**–**115** (2014) 61–68.

[6] I. Galić, K. Vučković, Z. Tonković, Nonlinear numerical analysis of two-way globe valve housing, Tech. Gaz. **17** (2010) 67–74.

[7] A. Milovanovic, A. Sedmak, R. Tomic, I. Hot, I. Martic, Calculation of local loads in torispherical end of vertical vessel with skirt according to EN 13445-3:2014, Structural Integ. Life, **16** (2016) 53–58.

[8] I. Dimic, N. Tomovic, J. Blazic, M. Rakin, B. Bugarski, Strength design calculation of a horizontal pressure vessel, Structural Integ. Life **13** (2013) 157–161.

[9] J. Orteu, 3-D computer vision in experimental mechanics, Opt. Lasers Eng. **47** (2009) 282–291.

[10] B. Pan, D. Wu, L. Yu, Optimization of a three-dimensional digital image correlation system for deformation measurements in extreme environments, Appl. Opt. **51** (2012) 440–449.

[11] M. Sutton, J. Orteu, W. Hubert, Image Correlation for Shape, Motion and Deformation Measurements: Basic Concepts, Theory and Applications, Springer, Berlin, 2009.

[12] M. Vautrot, P. Balland, O.S. Hopperstad, L. Tabourot, J. Raujol-Veillé, F. Toussaint, Experimental Technique to Characterize the Plastic Behaviour of Metallic Materials in a Wide Range of Temperatures and Strain Rates: Application to a High-Carbon Steel, Exp. Mech. **54** (2014) 1163–1175.

[13] P. Wang, F. Pierron, O.T. Thomsen, Identification of Material Parameters of PVC Foams using Digital Image Correlation and the Virtual Fields Method, Exp. Mech. **53** (2012) 1001–1015.

[14] G. Subhash, Q. Liu, D. F. Moore, P.G. Ifju, M.A. Haile, Concentration Dependence of Tensile Behavior in Agarose Gel Using Digital Image Correlation, Exp. Mech. **51** (2011) 255–262.

[15] N. Turton, S.Y. Jin, A. Majumder, H. An, V. Vijayan, W. Altenhof, D. Green, Experimentally Observed Strain Distributions Near Circular Discontinuities of AA6061-T6 Extrusions During Axial Crush, Exp. Mech. **51** (2011) 111–129.

[16] D. Lee, H. Tippur, P. Bogert, Dynamic fracture of graphite/epoxy composites stiffened by buffer strips: An experimental study, Compos. Struct. **94** (2012) 3538––3545.

[17] M. Milosevic, N. Milosevic, S. Sedmak, U. Tatic, N. Mitrovic, S. Hloch, R. Jovicic, Digital image correlation in analysis of stiffness in local zones of welded joints, Technical Gazette **23** (2016) 19–24.

[18] Lj. Tihacek-Sojic, A. Milic Lemic, I. Tanasic, N. Mitrovic, M. Milosevic, A. Petrovic, Compressive strains and displacement in a partially dentate lower jaw rehabilitated with two different treatment modalities, Gerodontology **29** (2012) 851–857.

[19] I. Tanasic, A. Milic-Lemic, Lj. Tihacek-Sojic, I. Stancic, N. Mitrovic, Analysis of the compressive strain below the removable and fixed prosthesis in the posterior mandible using a digital image correlation method, Biomech. Model. Mechanobiol. **11** (2012) 751–758.

[20] P. Sztefek, M. Vanleene, R. Olsson, R. Collinson, A. Pitsillides, S. Shefelbine, Using digital image correlation to

determine bone surface strains during loading and after adaptation of the mouse tibia, J. Biomech. **43** (2010) 599–605.

[21] G. Machado, D. Favier, G. Chagnon, Membrane Curvatures and Stress-strain Full Fields of Axisymmetric Bulge Tests from 3D-DIC Measurements. Theory and Validation on Virtual and Experimental results, Exp. Mech. **52** (2012) 865–880.

[22] B. Ahn, J. Kim, Measurement and characterization of soft tissue behavior with surface deformation and force response under large deformations, Med. Image Anal. **14** (2010) 138–148.

[23] T. Sadowski, L. Marsavina, E.M. Craciun, M. Kneć, Modelling and experimental study of parallel cracks propagation in an orthotropic elastic material, Comput. Mater. Sci. **52** (2012) 231–235.

[24] J.J. Hu, G.W. Chen, Y.C. Liu, S.S. Hsu, Influence of Specimen Geometry on the Estimation of the Planar Biaxial Mechanical Properties of Cruciform Specimens, Exp. Mech. **54** (2014) 615–631.

[25] M. Balac, A. Grbovic, A. Petrovic, Numerical predictions of crack growth in a pressure vessel with welded nozzles, Structural Integ. Life **15** (2015) 55–61.

[26] R. Zhang, L. He, Measurement of mixed-mode stress intensity factors using digital image correlation method, Opt. Lasers Eng. **50** (2012) 1001–1007.

[27] Q. Lin, J.F. Labuz, Fracture of sandstone characterized by digital image correlation, Int. J. Rock Mech. Min. Sci. **60** (2013) 235–245.

[28] F. Hild, S. Roux, Digital Image Correlation: from Displacement Measurement to Identification of Elastic Properties – a Review, Strain **42** (2006) 69–80.

IZVOD

EKESPERIMENTALNA I NUMERIČKA ANALIZA KUĆIŠTA RAVNOG ZAPORNOG VENTILA

Nenad R. Mitrovic[1], Aleksandar Lj. Petrovic[1], Milos S. Milosevic[2], Nikola V. Momcilovic[1], Zarko Z. Miskovic[1], Tasko Dj. Maneski[1], Predrag S. Popovic[3]

[1]*Univerzitet u Beogradu, Mašinski fakultet, Kraljice Marije 16, 11000 Beograd, Srbija*
[2]*Univerzitet u Beogradu, Inovacioni Centar Mašinskog fakulteta, Kraljice Marije 16, 11000 Beograd, Srbija*
[3]*Univerzitet u Beogradu, Institut za nuklearne nauke Vinča, Mike Petrovića Alasa 12-14, 11000 Beograd, Srbija*

(Naučni rad)

Eksperimentalna analiza kompleksnih struktura je uvek predstavljala veliki izazov za istraživače. Konvencionalne eksperimentalne metode (npr. merne trake) pružaju samo ograničene količine podataka u pogledu merenja na kritičnim mestima velikih geometrijskih diskontinuiteta. Metoda 3D korelacije digitalnih slika je optička metoda koja prevazilazi ograničenja konvencionalnih metoda i omogućava merenje kompletnog polja pomeranja i deformacija geometrijski kompleksnih struktura. Sistem Aramis, koji je baziran na metodi korelacije digitalnih slika, je korišćen za eksperimentalnu analizu i verifikaciju numeričkog modela u okviru ovog rada. Kompleksna struktura koja je analizirana u toku rada je spoj sfere i cilindra na kućištu ravnog zapornog ventila opterećenog aksijalnom silom. Najveće izmerene vrednosti Mizesovih deformacija iznse 0,15% na spoju sfere i cilindra. Vrednosti Mizesovih deformacija na cilindričnom i sfernom delu su i nekoliko puta manje nego na samom spoju. Važno je naglasiti da je, koliko je autorima poznato, ovo prvi rad koji prikazuje eksperimentalno određeno 3D deformaciono polje geometrijski kompleksne strukture (spoj sfere i cilindra) na samom spoju na opremi pod pritiskom. Pokazano je da je metoda 3D korelacije digitalnih slika brza i prilagodljiva metoda za merenje deformacija u toku opterećivanja kompleksnih struktura.

Ključne reči: Geometrijski diskontinuitet • Kućište ravnog zapornog ventila • Metoda 3D korelacije digitalnih slika • Metoda konačnih elemenata • Spoj sfere i cilindra • Aksijalno opterećenje